Transesterification reaction for biodiesel production from soybean oil using $Ni_{0.5}Zn_{0.5}Fe_2O_4$ nanomagnetic catalyst: Kinetic study

António B. Mapossa[1,2*], Joelda Dantas[1], Ana Cristina F.M. Costa[1]

[1]Federal University of Campina Grande, Synthesis of Ceramic Materials Laboratory – LabSMaC, Science and Engineering of Materials Postgraduate, Aprígio Veloso Avenue – 882, Bodocongó, Zip Code 58109-970 Campina Grande, PB, Brazil

[2]Institute of Applied Materials, Department of Chemical Engineering, University of Pretoria, Private Bag X20, Hatfield 0028, Pretoria, South Africa

Correspondence*: mapossabenjox@gmail.com

HIGHLIGHTS

- $Ni_{0.5}Zn_{0.5}Fe_2O_4$ catalyst was synthesized by combustion method
- Important reaction parameters were evaluated
- Transesterification reaction kinetic for soybean oil and methanol was determined
- Biodiesel was produced by transesterification method using $Ni_{0.5}Zn_{0.5}Fe_2O_4$ catalyst

SUMMARY

Biodiesel was successfully produced by transesterification process of soybean oil and methanol using $Ni_{0.5}Zn_{0.5}Fe_2O_4$ nanomagnetic catalyst. The $Ni_{0.5}Zn_{0.5}Fe_2O_4$ catalyst was synthesized by the combustion method and its properties were investigated using X-ray diffraction (XRD), N_2 physisorption at 77 K, Fourier transform infrared analysis (FT-IR), Thermogravimetric analysis (TGA), scanning electron microscopy (SEM) and a transmission electron microscopy (TEM). The performance of catalyst was investigated during transesterification reaction for FAMEs production. Fatty acid methyl esters (FAMEs) were studied by gas chromatography (GC) technique. The effect of reaction conditions such as molar ratio of methanol/soybean oil, catalyst amount, reaction temperature and reaction time on FAMEs yield were also evaluated. The biodiesel yield of 92.1 % was obtained under the following reaction conditions: 9:1 of methanol/soybean oil molar ratio and, 2 % of catalyst loading at 180 °C in 3 h. Furthermore, the energy of activation (Ea) was 67.4 kJ.mol^{-1} and the pre-exponential factor (k_o) was 8.35×10^4 L mol^{-1} min^{-1} determined using Arrhenius equation.

KEYWORDS: Biodiesel, transesterification reaction, $Ni_{0.5}Zn_{0.5}Fe_2O_4$, kinetic model

1 INTRODUCTION

Biodiesel is a renewable fuel that can be produced from vegetable oils, animal fats, and cooking oils as raw material in the presence of a short chain alcohol such as methanol or ethanol. For this, different methods for biodiesel production are used, for example; micro-encapsulation,

esterification, pyrolysis, and transesterification.[1-3] Among them, transesterification method is preferred for the reason that it produces biodiesel with low viscosity and its combustion characteristics are near to fuel produced from diesel.[3] Methanol is an alcohol preferred since it is inexpensive and has excellent physical and chemical properties, such as, a higher reactivity due to methanol being a polar molecule.[3-5] Further, However, homogenous catalysts are very much applied on transesterification process, but one of the shortcoming associated with homogenous catalysts is that, homogeneous catalysts are very difficult to separate from the components of mixture during reaction and must be neutralized and washed at the end of reaction, hence, creating difficulties in separation and recycling of spent catalysts.[6-8] This is also supported by Vahid et al.[43] when they reported the problems of using homogenous acid catalyst such as H_2SO_4 and HCl associated with the excessive time required to perform the reaction, corrosion and high separation costs.

In response to this problem, the development of heterogeneous catalysts for biodiesel production is gaining much attention from many researchers due the advantages of heterogeneous catalysts obtained at nanometric scale added to the magnetic property, constitute an appropriate and pertinent contribution to the chemical reactions of transesterification for biodiesel production. Therefore, these heterogeneous catalysts can be easily separated, regenerated, and reused for the further cycle during transesterification process.[11,44]. Thus, it reduces the contamination to the environment because lower amount of waste is generated during this process. In addition, heterogeneous catalysts become even more advantageous when they are spinel-type, since they allow a great cationic mobility, where their original crystalline structure may have substitution of chemical elements for other elements of same structure, that are similar in terms of electronegativity, valence, and radius size.[15] Most recently spinels such as $NiFe_2O_4$,[9]

$Ni_{0.3}Zn_{0.7}Fe_2O_4$,[9] $CoFe_2O_4$,[12] $ZnFe_2O_4$,[14] $Ni_{0.5-x}Cu_{0.5-x}Zn_{0.5}Fe_2O_4$,[15] $Ni_{0.7}Zn_{0.3}Fe_2O_4$,[42] have been used in the biodiesel production. However, the spinel ferrites can present support for the catalyst of biodiesel production due of their excellent properties such as large surface area and high thermal resistance. The method of synthesis plays a principal role in physicochemical properties of nanomagnetic catalyst obtained.[9,13,43] However, in order to produce these materials, various chemical methods of preparation have been reported as follow; solid-state reaction[16], solid-state reaction by microwave[17,18], sonochemical process[19], precursor citrate[20], precipitation[21], sol-gel[22], co-precipitation[23] and combustion reaction.[9,13,15] From the literature among the aforementioned chemical techniques, combustion technique has more advantages such as simplicity and short time required to produce a catalyst with a higher porosity.[24-26,43] Therefore, in our study, the combustion method can be an appropriate method to prepare a nanomagnetic catalyst for biodiesel production. The kinetic study of transesterification process of oil and methanol catalyzed by alkali has been reported in literature.[27,29,30] The kinetic study offers parameters i.e. the activation energy (Ea), to estimate the reaction velocity as a function of time under conditions.[27,28] However, to the best of our knowledge, the kinetic study of $Ni_{0.5}Zn_{0.5}Fe_2O_4$ nanomagnetic catalyst in transesterification reaction has not yet been explored. In our current study, the main objective was to investigate the kinetic of biodiesel production from soybean oil/methanol using $Ni_{0.5}Zn_{0.5}Fe_2O_4$ as a nanomagnetic catalyst by optimizing the parameters such as oil to methanol ratio, catalyst concentration, reaction temperature and reaction time. To support this objective, the properties of prepared catalyst were investigated by various techniques of characterization such as X-ray diffraction spectroscopy, BET textural analysis, Fourier transform infra-red spectroscopy, thermogravimetric analysis, scanning electron microscopy, transmission electron microscopy, zeta potential and acidity analysis and by a vibrating sample magnetometer analysis.

2 EXPERIMENTAL

2.1 Materials

To synthesize $Ni_{0.5}Zn_{0.5}Fe_2O_4$ catalysts, the following chemicals were used: nickel nitrate hexahydrate ($Ni(NO_3)_2.6H_2O$) with 98 % of purity supplied by Vetec. Zinc nitrate hexahydrate ($Zn(NO_3)_2.6H_2O$) with purity of 97% supplied by Vetec. Iron (III) nitrate nonahydrate - $Fe(NO_3)_3.9H_2O$ (purity, 99%) supplied by Vetec. Urea - $[(NH_2)_2CO]$ (purity, 97%) was supplied by Vetec. For biodiesel production the chemicals used were: Methanol – CH_3OH (purity, 99 %) supplied by Sigma-Aldrich and soybean oil refined was purchased in Campina Grande/Brazil. The physic-chemical properties result of soybean oil refined was previously published.[9]

2.2 Catalyst Preparation

The $Ni_{0.5}Zn_{0.5}Fe_2O_4$ nanomagnetic catalyst was prepared via combustion technique. The choice of this combustion method was due to the great advantage compared with other synthesis methods of catalysts as previously reported in the introduction section. The combustion method is represented by Equation (1):

$$0.5Ni(NO_3)_2.6H_2O_{(s)}+0.5Zn(NO_3)_2.6H_2O_{(s)}+2Fe(NO_3)_3.9H_2O_{(s)}+6.67(NH_2)_2CO_{(s)}\rightarrow$$

$$Ni_{0.5}Zn_{0.5}Fe_2O_{4(s)}+6.67CO_{2(g)} + 37.33H_2O_{(g)} + 10.67N_{2(g)} \quad \text{(Equation 1)}$$

2.3 Characterization of catalyst

The structural characteristics, identifications of phases and determination of crystallite size and crystallinity of the catalyst was investigated using X-ray diffraction, model Shimadzu XRD 6000 (CuKa radiation source, $\lambda = 1.542$ Å, a voltage of 40 kV, current of 30 mA and scanning between 20 - 70 ^{o}C). The size of crystallite was determined by Scherrer equation.[31]

BET textural analysis using gas N_2 adsorption, model 3200E YOUNG, Quantachrome® was used to check the textural characteristics of $Ni_{0.5}Zn_{0.5}Fe_2O_4$. With this method, the specific surface area of samples was determined, and the size of particles was determined by Reed formula.[32]

FTIR spectra were recorded on a Perkin-Elmer Spectrum 100 instrument in ATR mode. The spectra represent averages of 16 scans scanned at a resolution of 4 cm^{-1}. TGA/DTG analysis on a TA Instruments SDT-Q600 Simultaneous TGA/DSC was used to investigate the thermal stability of catalyst. SEM was used to investigate the morphological properties of $Ni_{0.5}Zn_{0.5}Fe_2O_4$ catalyst. The samples were viewed through a Shimadzu Corporation-(Superscan SSX-550 Scanning Electron Microscopy-Energy Dispersion X-Ray). Additionally, Transmission Electron Microscopy, a model JEM-3010, JEOL-300kv, was also used to investigative the morphology of catalyst. The Vibrating Sample Magnetometer, a model 7404 using Lake Shore, was used to determine the magnetic characteristic of catalyst. The active sites analysis was investigated by temperature desorption (TPD) method using NH_3 molecules. In TPD-NH_3 studies, the catalyst was subjected to a heating under temperature and flow schedule of an inert gas before equilibrated with a gas under well-defined temperature and partial pressure conditions. The flow gas that flows out on the sample is monitored by the continuous gas desorption.[9]

2.4 Transesterification reaction

In the transesterification reaction the following conditions were evaluated: (i) Methanol/ oil molar ratio 3:1, 6:1 and 9:1; (ii) 0.5; 1; 1.5 and 2 % of catalyst; (iii) reaction temperature (140; 160 and 180 ºC) and (iv) reaction time (1; 2; 3 and 4 h). The results of the parameters are reported in triplicate and discussed. The reaction conditions were investigated with the objective of getting a high yield of biodiesel. After the reaction, the nanocatalyst was separated from FAMEs and glycerol using a magnetic field (Figure 5a). The mixture of the components of FAMEs and a small

amount of glycerol were separated by decantation and further using centrifugation during 40 min at 9000 RPM to promote a total separation of the components of mixture via sedimentation. Biodiesel was analyzed using the gas chromatograph (GC) technique, model VARIAN 450c. The formula represented by Equation 2,[38] was used to determine the biodiesel mass yield.

$$Mass\ yield\ (\%) = \frac{Weight\ of\ biodiesel}{Weight\ of\ oil} \times 100 \qquad (2)$$

2.5 Transesterification reaction kinetic study

Equation (2) illustrates the general transesterification reaction using methanol. In general, the triglyceride (TG) is reversible. To conduct the reaction to the products side and to obtain esters, a higher methanol/oil molar ratio of 9:1 was required compared to the stoichiometric of methanol/oil molar ration (3:1) (Equation 3). In this work, the influence of reverse reaction and methanol concentration was negligible.[28,33,34] The kinetic of transesterification reaction follows the pseudo-first-order as is shown by Equation (4).[37]

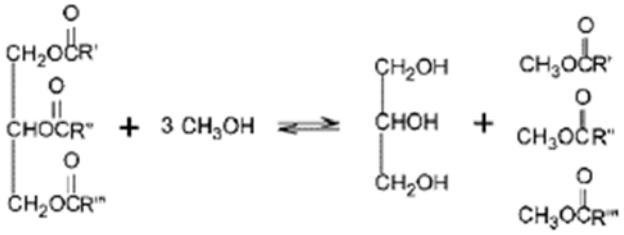

Equation 3. Transesterification reaction of triglycerides with methanol.[39]

$$r = -\frac{d[TG]}{dt} = k[TG][M]^3 \qquad (4)$$

where *[TG]* represents the triglyceride concentration and *[M]* is a concentration of methanol, both in (mol/L).

$$k' = k[M]^3 \qquad (5)$$

By integration of Equation (2), it offers:

$$\ln[TG,t] - \ln[TG,t] = k't \tag{6}$$

$$k' = \frac{\ln[TG,0] - \ln[TG,t]}{t} \tag{7}$$

In addition,

$$[TG,t] = [TG,0] - \frac{[FAMEs,t]}{3} \tag{8}$$

Where, k represents constant rate in L.mol^{-1}.min^{-1}, the time of reaction is represented by t in (min). The concentrations of triglyceride and fatty acid methyl esters as a function of time are represented by [TG, t], [TG, 0] and [FAMEs] in (mol/L). The [Biodiesel, t] can be obtained from GC analysis. By fitting of Equation (3), the k values were determined at different temperatures. The Arrhenius formula represented by Equation (9) was used to calculate the activation energy. [28,34] As it is known that the activation energy plays a role to accelerate the velocity of transesterification reaction for the formation of fatty acid methyl esters (FAMEs).

$$k = k_0 \, x \, e^{-\frac{E_a}{RT}} \tag{9}$$

By integration, it can be transformed as follows:

$$lnk = -\frac{E_a}{RT} + lnk_0 \tag{10}$$

Where, the activation energy (Ea) is represented in (KJ/mol); the constant of gas (R) corresponds (8.314 J.mol^{-1}/K while the temperature (T) is in kelvin (K), and the pre-exponential factor (k_o) is in (L.mol^{-1}.min^{-1}).

3 RESULTS AND DISCUSSION

3.1 Catalyst Characterization

3.1.1 XRD analysis and BET analysis

XRD patterns of $Ni_{0.5}Zn_{0.5}Fe_2O_4$ in triplicate are shown in Figure 1. The formation of a single crystalline phase of the inverse spinel with space group *Fd3m* was observed. No other phases were detected. The spinel phase was identified by the standard card JCPDF 52-0278. The catalyst showed diffraction peaks with a considerably basal width, indicating the nanosized characteristic of particles of the synthesized material. Further, the catalyst exhibited 17 nm of crystallite size and 80 % of crystallinity, demonstrating that the combustion method used in this study was effective. The adsorption/desorption isotherm of $Ni_{0.5}Zn_{0.5}Fe_2O_4$ is shown in Figure 2. The catalyst had an isotherm type V, typical of mesoporous materials.[36] The mesoporous enhanced the performance of the catalyst. According to the research work conducted by Mohamed et al. [38] the diffusion of free fatty acid inside and outside of the catalyst is generated by mesopores. The catalyst presented hysteresis loop type H3 as is reported in Figure 2. Furthermore, the $Ni_{0.5}Zn_{0.5}Fe_2O_4$ catalyst exhibited a reasonable specific surface area (BET) of 74.42 ± 0.71 m^2g^{-1}, particle size (D_{BET}) of 15 ± 0.41 nm, volume of pores (Vp) of 0.168 ± 0.02 cm^3/g and pore radius Dv(r) = 37.484 Å, respectively.

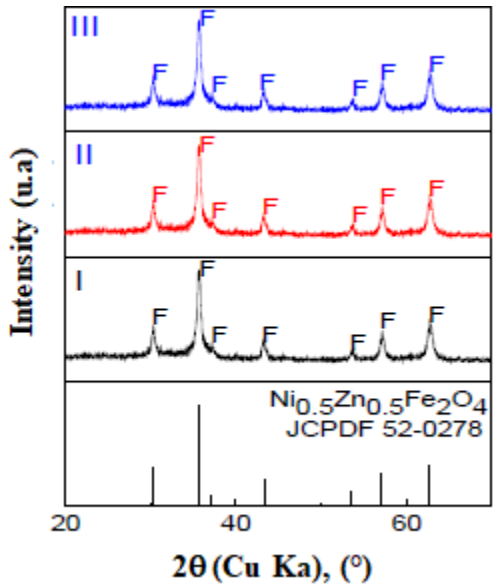

FIGURE 1 XRD patterns of $Ni_{0.5}Zn_{0.5}Fe_2O_4$ catalyst

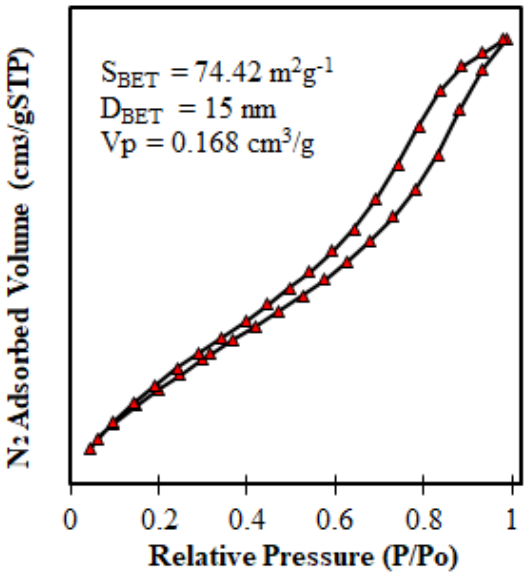

FIGURE 2 Adsorption / desorption isotherms of $Ni_{0.5}Zn_{0.5}Fe_2O_4$ catalyst

3.1.2 FTIR and TGA analysis

FTIR spectra of $Ni_{0.5}Zn_{0.5}Fe_2O_4$ in range 700 – 400 cm^{-1} is shown in Figure 3. Two bands demonstrating tetrahedral and octahedral sites were observed approximately at 578 cm^{-1} and 430

cm^{-1}. Figure 4 shows traces for the $Ni_{0.5}Zn_{0.5}Fe_2O_4$ investigated by TGA/DTG. However, the catalyst featured three stages thermal degradation. The first step for the $Ni_{0.5}Zn_{0.5}Fe_2O_4$ had onset temperatures of 31 ºC while the maximum rate occurred at 198 ºC. This is attributed the initial breakdown of the complex and spontaneous combustion and evaporation of absorbed water.[9] The corresponding values for the second step were 200 ºC for the onset temperatures and 350 ºC for the maximum mass loss rate. This is attributed to the oxidation and decomposition of the organic material of inorganic salts.[35] The third stage is between 445 ºC to 550 ºC demonstrating the formation of corresponding metal. No mass loss was observed above of 578 ºC, this suggests that: (i) the thermal decomposition was completed; and (ii) the $Ni_{0.5}Zn_{0.5}Fe_2O_4$ catalyst was formed.

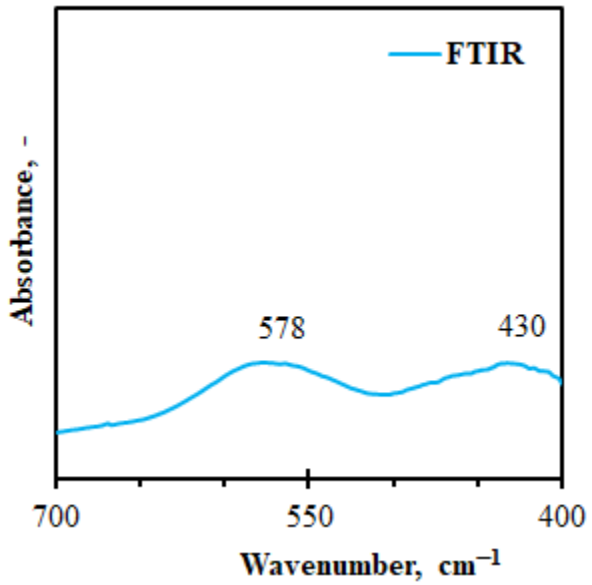

FIGURE 3 FTIR spectra of $Ni_{0.5}Zn_{0.5}Fe_2O_4$ catalyst

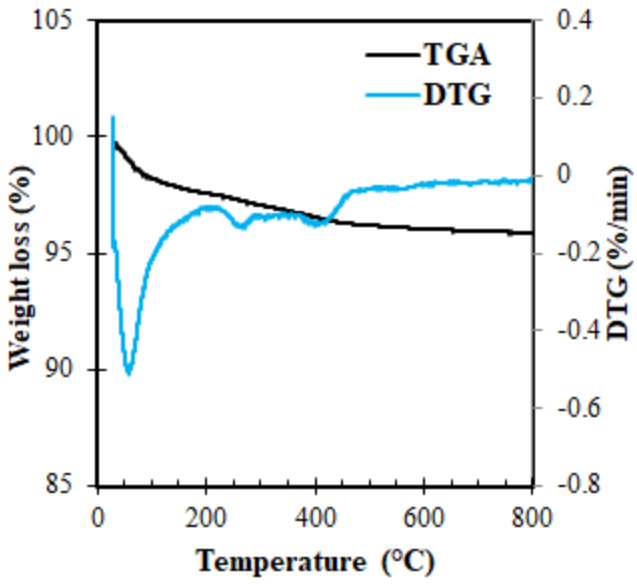

FIGURE 4 TGA/DTG analysis of $Ni_{0.5}Zn_{0.5}Fe_2O_4$ catalyst

3.1.3 Zeta potential and pH in catalytic activity

The zeta potential informs about the electric charges on the surface of the solid, which is a feature of the change of acidity in the material due to absorption and desorption of ions and protons. Therefore, the Zeta potential and pH values were 12 ± 0.11 mV and 6.20 ± 0.34. This suggests that the catalyst had good stability and a positive surface charge.

3.1.4 TPD - NH_3 analysis

The acid sites are related to the interaction force present in catalyst which is classified in three types: weak, moderate, and strong acid sites as listed in Table 1. Figure 5 shows the acid sites of the $Ni_{0.5}Zn_{0.5}Fe_2O_4$ curves obtained by TPD - NH_3 analysis. The strong acid sites were observed at temperature range 307 – 448 ºC. While the moderate acid sites were observed at 170 ºC to 300 ºC and the last interval in the lower temperature range 100 – 168 ºC could be represent the weak acid

sites present on the surface of the $Ni_{0.5}Zn_{0.5}Fe_2O_4$. The strong acid sites influenced the transesterification reaction for biodiesel production.

TABLE 1 Acid sites of the synthesized $Ni_{0.5}Zn_{0.5}Fe_2O_4$ catalyst

Catalyst	Weak acid sites ($mL.g^{-1}$)	Moderate acid sites ($mL.g^{-1}$)	Strong acid sites ($mL.g^{-1}$)
$Ni_{0.5}Zn_{0.5}Fe_2O_4$	0.52	1.14	1.73

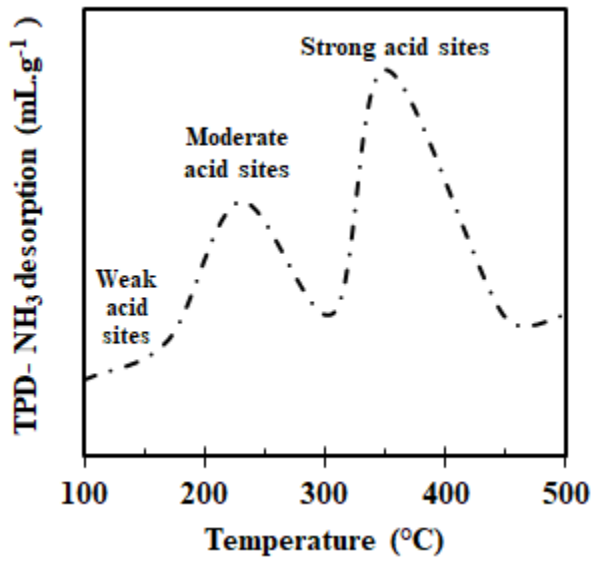

FIGURE 5 Curves of acid sites of the $Ni_{0.5}Zn_{0.5}Fe_2O_4$ obtained by TPD - NH_3 analysis

3.1.5 SEM and TEM analysis studies

Figure 6 shows SEM micrographs of the $Ni_{0.5}Zn_{0.5}Fe_2O_4$ catalyst. The mesoporous structures of the nanomagnetic catalyst were confirmed using SEM. The particle agglomeration with varied forms and dimensions is clearly visible. The ions Ni^{2+} and Zn^{2+} affected the morphology of catalyst synthesized. Additionally, the confirmation of the weak agglomeration of the interconnected particles with various forms were observed using TEM and as shown in Figure 7. The agglomeration of particles is due to the combustion method used to synthesize $Ni_{0.5}Zn_{0.5}Fe_2O_4$ catalyst.

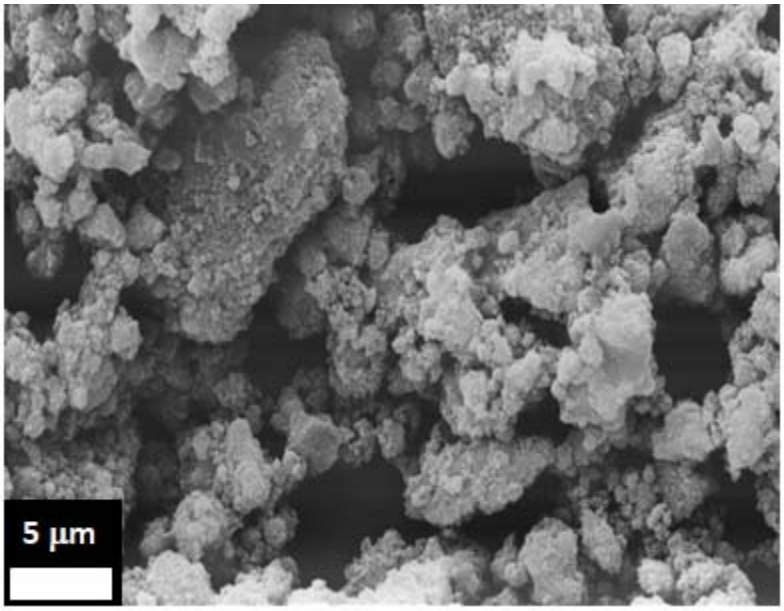

FIGURE 6 SEM image of $Ni_{0.5}Zn_{0.5}Fe_2O_4$ catalyst

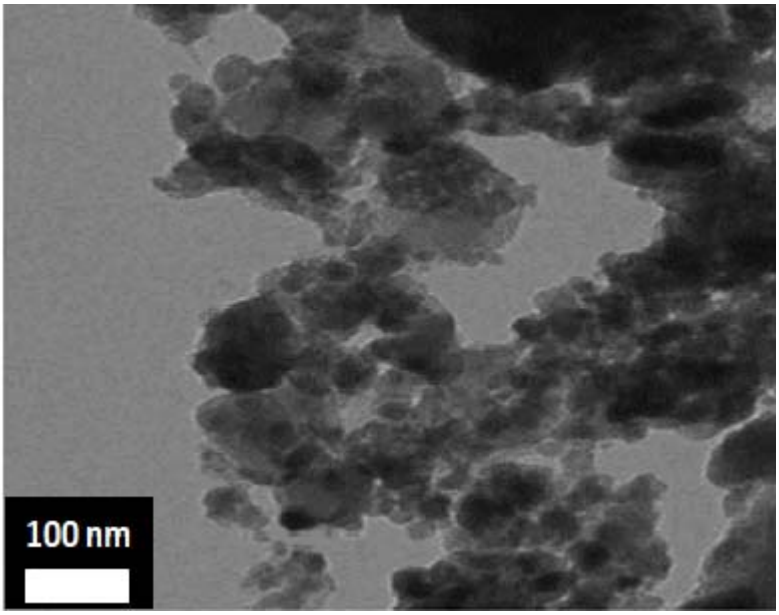

FIGURE 7 TEM image of $Ni_{0.5}Zn_{0.5}Fe_2O_4$ catalyst

3.1.6 Magnetic property via VSM

The $Ni_{0.5}Zn_{0.5}Fe_2O_4$ magnetic property is presented in Figure 8. The catalyst revealed the magnetic hysteresis with a well-defined and narrow *S* format, indicating ferromagnetic behavior, characteristic of soft magnetic materials.[13,15] The $Ni_{0.5}Zn_{0.5}Fe_2O_4$ presented a reasonable

saturation value of magnetization, remnant value of magnetization and coercive force value which were of 30.47 ± 0.97 emu/g, 1.71 ± 0.17 and 45.12 ± 1.04, respectively. Additionally, Figure 9 illustrates images of the excellent magnetic response of the $Ni_{0.5}Zn_{0.5}Fe_2O_4$. The nanomagnetic catalyst used in transesterification reaction responds well to the magnet that produces a magnetic field. This suggests that after reaction the catalyst could be separated from components to ensure its reuse.

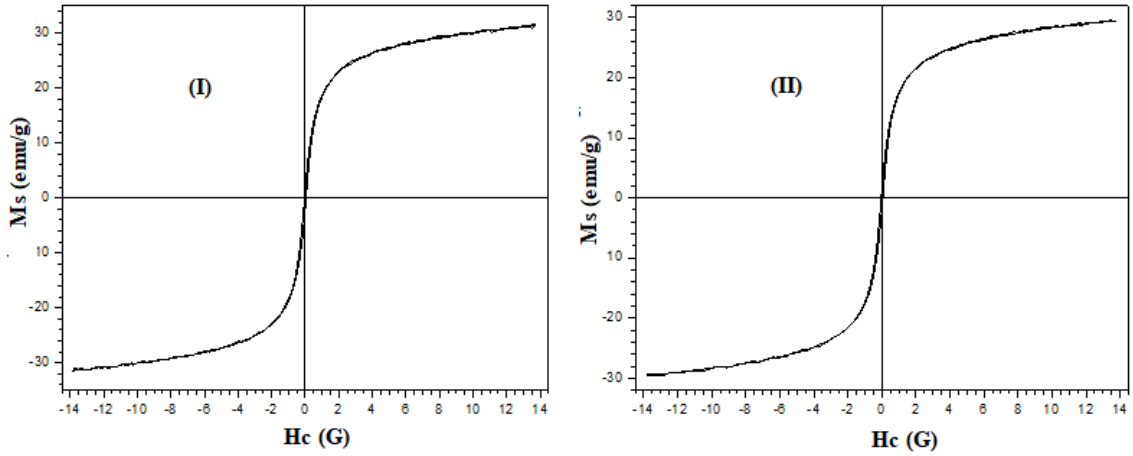

FIGURE 8 Hysteresis curves M x H in duplicate (I and II) of the $Ni_{0.5}Zn_{0.5}Fe_2O_4$

FIGURE 9 $Ni_{0.5}Zn_{0.5}Fe_2O_4$ nanomagnetic catalyst during transesterification reaction and separation process by magnet stimulus.[41]

3.2 Factors affecting transesterification reaction

3.2.1 Effect of catalyst on biodiesel yield

The effect of a catalyst on the yield of biodiesel is shown in Figure 10 (a). In this study, the catalyst evaluated was within the range of 0.5 -2 wt-% . The nanocatalyst loading during reaction induced for higher level of biodiesel production by enhancing the reaction rate. On 0.5 wt-% of catalyst loading, the reaction started slowly and achieved a high value of biodiesel yield of 71 % when the amount of catalyst was 2 wt-%. This is probably attributed to the acid sites. More loading of $Ni_{0.5}Zn_{0.5}Fe_2O_4$, can induce to the more acid sites, which is favorable on the performance of catalyst on transesterification reaction for higher biodiesel conversion. In this study, catalyst loading was not exceeded more than 2 wt-% . Dantas et al. [40] reported that the biodiesel yield was low when a higher concentration of catalyst loading of 4 wt-% was used. Furthermore, Zhang et al.[28] also reported that too much amount of catalyst increases the viscosity of the oil and alcohol mixture, consequently, it is difficult to get a good mixture and its separation. The results from this work suggest that catalyst concentration of 2 wt-% was enough to complete the biodiesel conversion in optimum reaction time. However, combining this parameter with others the best biodiesel yield can be achieved.

3.2.2 Effect of molar ration of methanol/oil on the yield of biodiesel

Figure 10 (b) shows the effect of the molar ratio of methanol/ oil on biodiesel yield investigated from 3:1 to 9:1. The results show that an increase in molar ratio increased the biodiesel yield reaching a maximum yield of 83 % with the molar ratio of 9:1. Lower molar ratio decreased the velocity of reaction kinetic as well as biodiesel yield while a higher molar ratio of 9:1 needed shorter reaction time to achieve a good yield. Similar findings were reported by researchers.[37] The aforementioned studies were done by Dantas et al.[40] which showed that the biodiesel yield was not

effective when too much molar ratio methanol/oil of 1:12 and 1:20. According to the literature[28], when too much molar ratio of methanol/soybean oil is used, it becomes difficult to separate glycerol from the mixture due to emulsion of glycerol with biodiesel, thereby decreasing the yield of biodiesel.

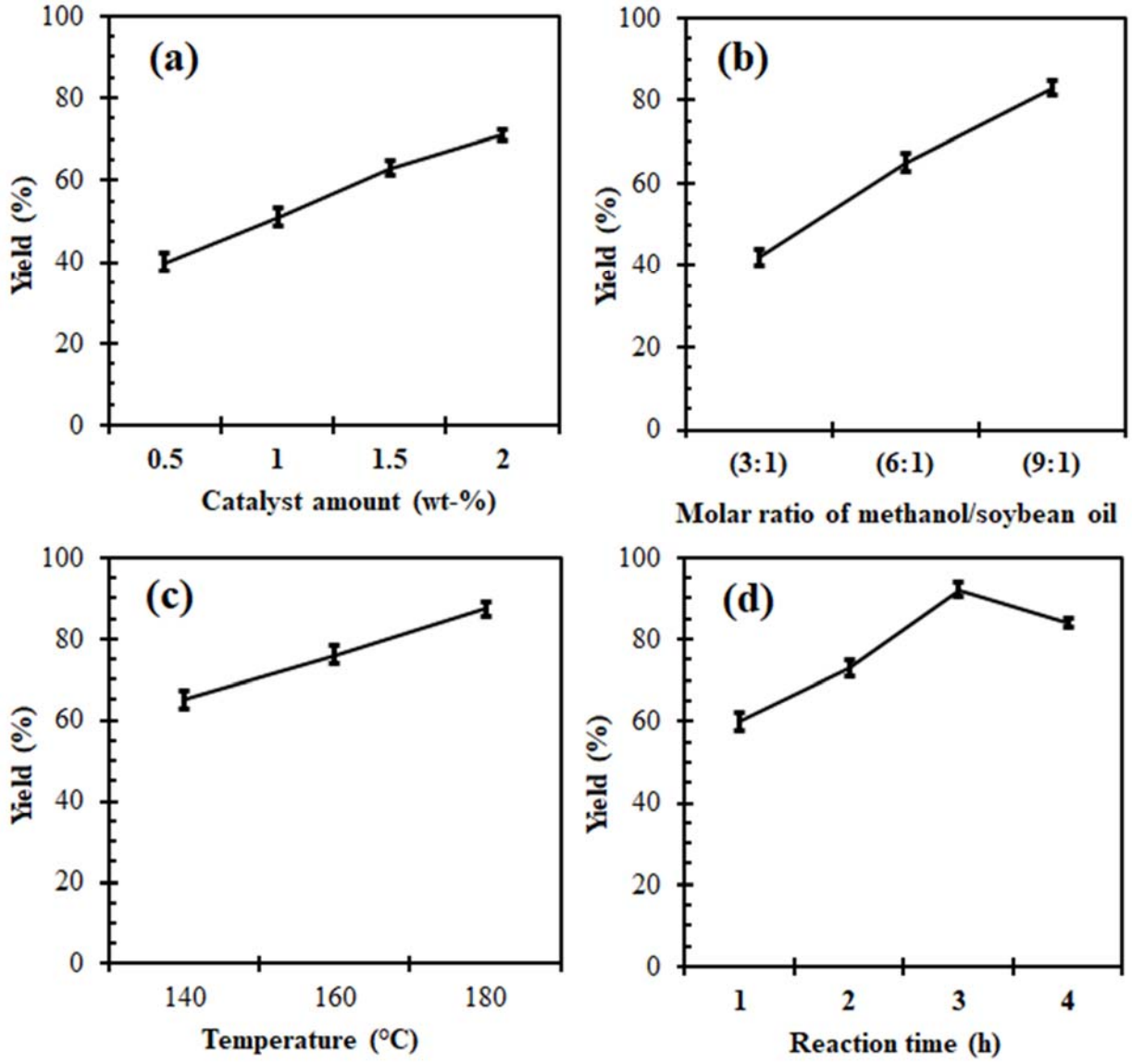

FIGURE 10 (a) Effect of catalyst amount on biodiesel yield (molar ratio of methanol/ soybean oil: 9:1; 3 h at 180 °C). (b) Effect of methanol/soybean oil molar ratio on biodiesel yield (catalyst: 2%; 3 h at 180 °C at). (c) Effect of temperature on biodiesel yield (methanol/soybean oil molar ratio: 9:1; catalyst: 2% at 3h. (d) Effect of time of reaction on biodiesel yield (methanol/soybean oil molar ratio: 9:1; catalyst: 2% at 180 °C).

3.2.3 Effect of temperature on the yield of Biodiesel

Figure 10 (c) shows effect of temperature on the yield of biodiesel. The biodiesel yield was enhanced with an increase in temperature. This is due to the reduction of soybean oil viscosity and an enhanced in miscibility with alcohol caused by increase in temperature. This also improves the contact of oil with alcohol and catalyst.[37] The best yield of biodiesel of 87.3 % was achieved at 180 °C. However, due low boiling point of methanol it also limits their use into most transesterification reaction because during processing at high temperatures, large amounts of alcohol can be lost by volatilization.

3.2.4 Effect of reaction time on biodiesel yield

Figure 10 (d) shows the trend of the effect of reaction time on biodiesel yield. The time of reaction was evaluated from 1 h to 4 h. Results show that increasing of time from 1 h to 3 h increased the biodiesel yield increased to 92.1%. But from 3 h to 4 h the yield decreased to 87 %. This is due to the transesterification reaction which is a reversible process which it conducts for reduction of higher yield of fatty acid methyl esters and production of soap.[38] However, the highest biodiesel yield of 92.1% was reached in 3 h. As is known, reaction time also plays a major role in transesterification reaction using heterogeneous catalysts.

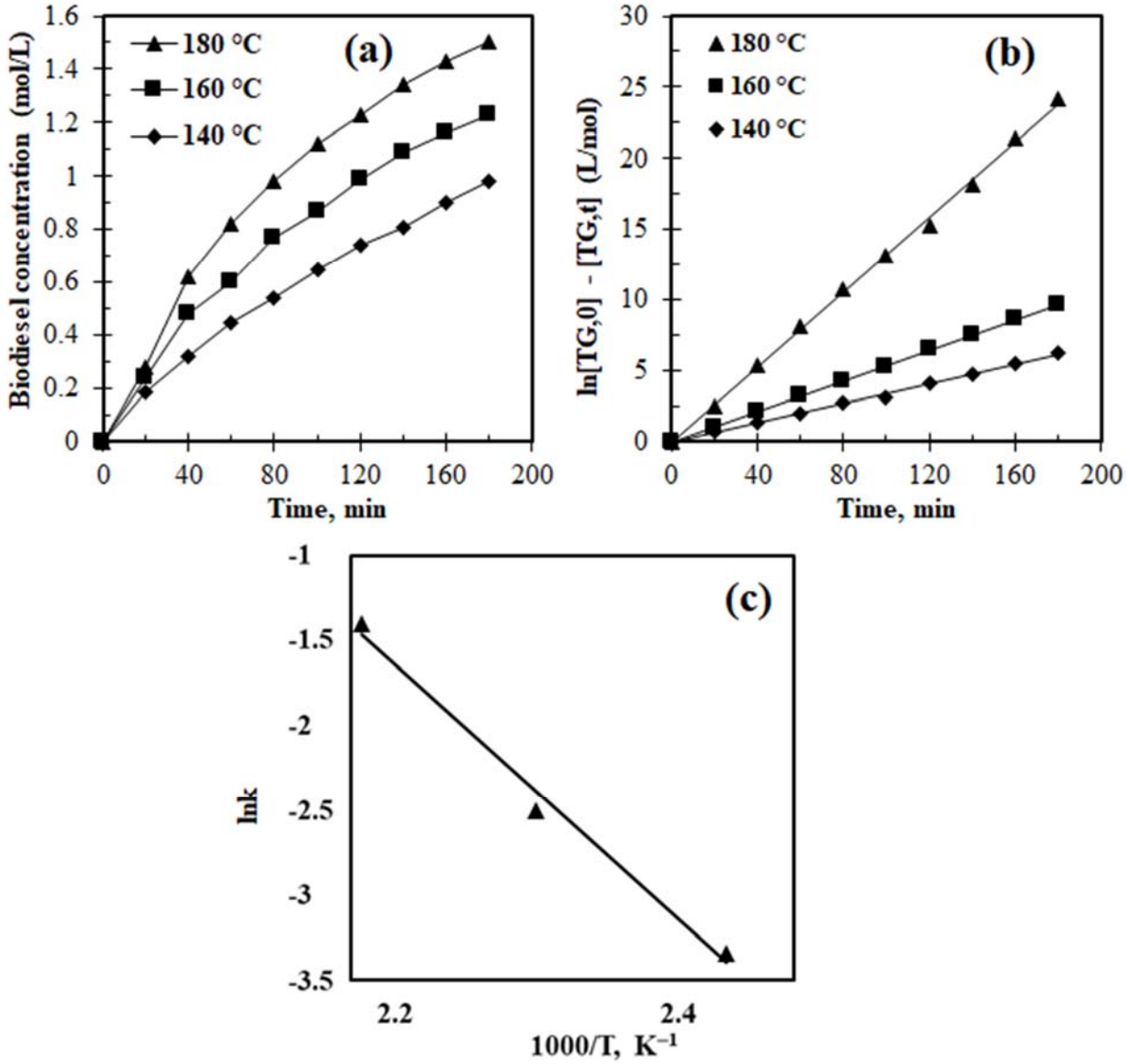

FIGURE 11 (a) Trends variation of concentration-time profile for biodiesel production at 140, 160 and 180 ºC under conditions: 9:1 of methanol/soybean oil molar ratio; 2% of catalyst. (b) Curve of linear regression of triglyceride concentration and time of reaction found by equation (3), under condition: 9:1 of methanol/soybean oil molar ratio; 2% of catalyst. (c) Prediction data of *lnk* as a function of *1/T* for the transesterification reaction for biodiesel production (9;1 of methanol/soybean oil molar ratio and 2 % of catalyst).

3.2.5 Reaction kinetics studies

Figure 11 (a) shows the variation trend of FAMEs concentration. The results demonstrate the trends that occur in three stages as a function of time: (i) initiation step is in range of 0–20 min, this shows a slow formation of fatty acid methyl esters (FAMEs); (ii) The second stage between 15 – 120 min is known as growth stage, where the fatty acid methyl esters were forming smoothly; (iii) finally, the last stage from 120 – 180 min, shows that the velocity of reaction to form FAMEs is too faster compared to the two previous stages. In this stage also the equilibrium is reached in around 180 min. Figure 11 (b) shows the fitting of experimental values as a function of temperatures of 140 ºC, 160 ºC and 180 ºC obtained by Equation (6). The excellent linear function plot of $ln[TG,0] - ln[TG, t]$ with time (t) was obtained. From curves in Figure 11 (b), it is visible to see that the experimental data is close to the predicted data. Table 2 lists the reaction rate constants (k) and correlation coefficients (R^2) at different temperatures. Note that the correlation coefficient obtained was greater than 0.996. Additionally, Arrhenius formula represented by Equation (9) was used to obtain the energy of activation. The values of energy of activation and the pre-exponential factor (k_o) were 67.4 kJ/mol and 8.35×10^4 L.mol^{-1}.min^{-1}. Figure 11 (c) shows excellent linearity observed between lnk and $1/T$ at different temperatures between 140 – 180 ºC. Furthermore, the experimental data is in close agreement with the predicted data. Finally, the Arrhenius equation of showing the reaction rate at a range of temperature 140 – 180 ºC was written as follows: $lnk = 20.45 - \frac{9875}{T}$.

TABLE 2 Lists of rates of constant (k) and correlation coefficients (R^2) of reaction as a function of temperature.

Temperature (ºC)	k (L.mol^{-1}.min^{-1})	R^2
140	0.0317	0.998
160	0.0955	0.997
180	0.2613	0.998

As a summary, the current work, suggests that, additional experimental exploration will be required to confirm the potential advantage of the conclusion reached herein. Clearly, it should be possible to produce biodiesel using nanomagnetic catalyst that is environmentally friendly. The best yield of FAMEs achieved in this work shows that they may be worthwhile to consider development of actual nanomagnetic catalysts based on the ferrites of spinel-type for large scale (industrial scale).

4 CONCLUSIONS

In this study, the $Ni_{0.5}Zn_{0.5}Fe_2O_4$ nanomagnetic catalyst was synthesized with the simple and applicable method of combustion for being used in biodiesel production. In transesterification reaction the synthesized catalyst showed the highest performance in the biodiesel production with a conversion of 92.1 %. The results of analyses presented that the presence of acid sites on surface of catalyst, suitable morphology, reasonable surface area and zeta potential of catalyst influenced in the biodiesel production. The kinetic studies were performed at different times and temperatures to find the rate constants suggesting that the reaction follows pseudo-first-order kinetics having activation energy and frequency factor as 67.4 kJ.mol^{-1} and 8.35×10^4 L mol^{-1} min^{-1} respectively. Evaluating the dependence of transesterification reaction in the biodiesel yield with the reaction parameters such as catalyst concentration, molar ratio of alcohol/oil, temperature and reaction time it was found that the optimum reaction conditions for biodiesel production were found to be methanol/oil molar ratio (9:1), catalyst concentration (2 wt%), temperature (180 °C) and the reaction time (3h). Finally, it can be said that the $Ni_{0.5}Zn_{0.5}Fe_2O_4$ nanomagnetic catalyst provides good potentials for industrialization due to its suitable performance in biodiesel production and environmentally friendly as well as its simple and inexpensive method of synthesis.

As for future work, the reusability of catalyst in transesterification process during biodiesel production will be explored. This is due to the catalyst excellent magnetic properties. Further, thereafter, its long-term use in transesterification reaction, the morphology, structure and composition of catalyst also will be investigated.

DECLARATION OF INTEREST

None

ACKNOWLEDGEMENTS

MCTM/CNPq [190822/2013-9] is thanked by authors for financial support. We also express our gratitude to Dr Gimo Daniel and Mr Robert Tewo for English reviewing the manuscript.

REFERENCES

1. Gui MM, Lee KT, Bhatia S. Feasibility of edible oil vs. non-edible oil vs. waste edible oil as biodiesel feedstock. Energy. 2008, 33(11),1646-1653.
2. Macor A, Pavanello P. Performance and emissions of biodiesel in a boiler for residential heating. Energy. 2009, 34(12),2025-2032.
3. Farooq M, Ramli A, Naeem A, Noman M, Shah LA, Khattak NS, Perveen F. A green route for biodiesel production from waste cooking oil over base heterogeneous catalyst. International Journal of Energy Research. 2019. DOI: 10.1002/er.4646.
4. Musa IA. The effects of alcohol to oil molar ratios and the type of alcohol on biodiesel production using transesterification process. Egypt J Pet. 2016;25(1):21-31.
5. Dai YM, Chen KT, Wang PH, Chen CC. Solid-base catalysts for biodiesel production by using silica in agricultural wastes and lithium carbonate.Adv Powder Technol. 2016;27(6):2432-2438.
6. Lopez DE, Goodwin Jr JG, Bruce DA, Lotero E. Transesterification of triacetin with methanol on solid acid and base catalysts. Applied Catalysis A: General. 2005; 295(2),97-105.
7. Liu Y, Zhang P, Fan M, Jiang P. Biodiesel production from soybean oil catalyzed by magnetic nanoparticle $MgFe_2O_4$@ CaO. Fuel. 2016; 164, 314-321.
8. Degirmenbasi N, Coskun S, Boz N, Kalyon D.M. Biodiesel synthesis from canola oil via heterogeneous catalysis using functionalized CaO nanoparticles. Fuel. 2015; 153, 620-627.
9. Mapossa AB, Dantas J, Silva MR, Kiminami RH, Costa ACF, Daramola MO. Catalytic performance of $NiFe_2O_4$ and $Ni_{0.3}Zn_{0.7}Fe_2O_4$ magnetic nanoparticles during biodiesel production. Arabian Journal of Chemistry. 2020; 13(2), 4462-4476.

10. Li Y, Qiu F, Yang D, Li X, Sun P. Preparation, characterization and application of heterogeneous solid base catalyst for biodiesel production from soybean oil. Biomass and bioenergy. 2011; 35(7), 2787-2795.

11. Baskar G, Selvakumari IAE, Aiswarya, R. Biodiesel production from castor oil using heterogeneous Ni doped ZnO nanocatalyst. Bioresource technology. 2018; 250, 793-798.

12. Zhang P, Han Q, Fan M, Jiang P. Magnetic solid base catalyst $CaO/CoFe_2O_4$ for biodiesel production: Influence of basicity and wettability of the catalyst in catalytic performance. Applied surface science. 2014; 317, 1125-1130.

13. Costa ACFM, Morelli MR, Kiminami RHGA. Combustion Synthesis: Effect of Urea on the Reaction and Characteristics of Ni-Zn Ferrite Powders. Journal of Materials Synthesis and Processing 2002a; 9:347-352.

14. Mapossa AB, Dantas J, Kiminami AGHR, Silva MR, Costa ACFM. Síntese do ferroespinélio $ZnFe_2O_4$ e avaliação do seu desempenho em reações de esterificação e transesterificação via rota metílica. Revista Eletrônica de Materiais e Processos. 2015; 10(3), 137-143.

15. Dantas J, Leal E, Mapossa AB, Cornejo DR, Costa ACFM. Magnetic nanocatalysts of $Ni_{0.5}Zn_{0.5}Fe_2O_4$ doped with Cu and performance evaluation in transesterification reaction for biodiesel production. Fuel. 2017; 191, 463-471.

16. Amiri GR, Yousefi MH, Abolhassani MR, Manouchehri S, Keshavarz MH, Fatahian S. Magnetic properties and microwave absorption in Ni–Zn and Mn– Zn ferrite nanoparticles synthesized by low-temperature solid-state reaction, Journal of Magnetism and Magnetic Materials 2011; 323:730–734

17. Gupta N, Verma A, Kashyap SC. Micro structural, dielectric and magnetic behavior of spin deposited nanocrystalline nickel-zinc ferrite thin films for microwave applications. Journal of Magnetism and Magnetic Materials 2007; 308:137-142.

18. Liu Y, Li J, Min F, Zhu J, Zhang M. Microwave-assisted synthesis and magnetic properties of $Ni_{1\_x}Zn_xFe_2O_4$ ferrite powder. Journal of Magnetism and Magnetic Materials 2014; 354:295-298.

19. Shafi K, Koltypin Y, Gedanken A, Prozorov R, Balogh J, Lendvai J, Felner I. Sonochemical preparation of nano-sized amorphous $NiFe_2O_4$ particles. Journal of Materials Chemistry and Physics 1997; 101:6409-6414.

20. Prasad S, Gajbhiye NS. Magnetic studies of nanosized nickel ferrite particles synthesized by citrate precursor technique. Journal of Alloys and Compounds 1998; 265:87-92.

21.Shi Y, Ding J, Liu X, Wang J. $NiFe_2O_4$ ultrafine particles prepared by co-precipitation/mechanical alloying. Journal of Magnetism and Magnetic Materials 1999; 205:249-254.

22. Chen DH, He XR. Synthesis of nickel ferrite nanoparticles by sol–gel method. Materials Research Bulletin 2001; 36:1369–1377.

23. Yang JM, Tsuo WJ, Yen FS. Preparation of ultrafine nickel ferrite powders using mixed Ni and Fe tartrates. Journal Solid State Chemistry 1999; 145:50-57.

24. Cai W, Fu C, Hu W, Chen G, Deng X. Effects of microwave sintering power on microstructure, dielectric, ferroelectric and magnetic properties of bismuth ferrite ceramics. Journal of Alloys and Compounds 2013; 554:64-71.

25. Costa ACFM, Kiminami RHGA, Morelli MR. Combustion synthesis processing of nanoceramics. In: Handbook of nanoceramics and their based nanodevices (Synthesis and Processing). Ed. American Scientific Publishers 2009; 1:375-392.

26. Ping R, Junxi Z, Huiyong D. Preparation and microstructure of spinel zinc ferrite $ZnFe_2O_4$ by co-precipitation method. Journal of Material Science 2009; 24: 927-930.

27. Darnoko D, Cheryan M. Kinetics of palm oil transesterification in a batch reactor. Journal of the American Oil Chemists' Society. 2000; 77(12),1263-1267.

28. Zhang L, Sheng B, Xin Z, Liu Q, Sun S. Kinetics of transesterification of palm oil and dimethyl carbonate for biodiesel production at the catalysis of heterogeneous base catalyst. Bioresource Technology. 2010; 101(21), 8144-8150.

29. Freedman B, Butterfield RO, Pryde EH. Transesterification kinetics of soybean oil. Journal of the American Oil Chemists' Society. 1986; 63(10),1375-1380.

30. Noureddini H, Zhu D. Kinetics of transesterification of soybean oil. Journal of the American Oil Chemists' Society. 1997; 74(11), 1457-1463.

31. Klung HP, Alexander LE. X-ray diffraction procedures. John Wiley & Sons, New York. 1962; 1, 974.

32. Reed J.S. Principles of ceramics processing. Second Edition, John Wiley & Sons, Inc., New York, NY (1995).

33. Ma F, Hanna MA. Biodiesel production: a review. Bioresource technology. 1999; 70(1),1-15.

34. Gao Y, Chen Y, Gu J, Xin Z, Sun S. Butyl-biodiesel production from waste cooking oil: Kinetics, fuel properties and emission performance. Fuel. 2019; 236,1489-1495.

35. Sivakumar P, Ramesh R, Ramanand A, Ponnusamy S, Muthamizhchelvan C. Preparation and properties of nickel ferrite (NiFe2O4) nanoparticles via sol–gel auto-combustion method. Materials Research Bulletin. 2011; 46(12), 2204-2207.

36. Sing KSW, Everett DH, Haul RAW, Moscou L, Pierotti RA, Rouquerol J, Siemieniewska T. Reporting physisorption data for gas/solid systems with special reference to the determination of surface area and porosity. Pure Applied of Chemistry. 1985; 57, 603–619.

37. Booramurthy VK, Kasimani R, Subramanian D, Pandian S. Production of biodiesel from tannery waste using a stable and recyclable nano-catalyst: An optimization and kinetic study. Fuel. 2020; 260,116373.

38. Mohamed, RM, Kadry GA, Abdel-Samad HA, Awad ME. High operative heterogeneous catalyst in biodiesel production from waste cooking oil. Egyptian Journal of Petroleum. Doi.org/10.1016/j.ejpe.2019.11.002.

39. Di Serio M, Tesser R, Pengmei L, Santacesaria E. Heterogeneous catalysts for biodiesel production. Energy & Fuels. 2007. 22(1),207-217.

40. Dantas J, Santos JRD, Silva FN, Silva AS, Costa ACFM. Study of nanoferrites $Ni_{0.5}Zn_{0.5}Fe_2O_4$ and $Ni_{0.1}Cu_{0.4}Zn_{0.5}Fe_2O_4$ as catalysts in the methyl transesterification of soybean oil. In Materials Science Forum. 2014; 775,705-711.

41. Dantas J, Leal E, Cornejo DR, Kiminami RHGA, Costa ACFM. Biodiesel production evaluating the use and reuse of magnetic nanocatalysts $Ni_{0.5}Zn_{0.5}Fe_2O_4$ synthesized in pilot-scale. Arabian Journal of Chemistry. 2020; 13(1), 3026-3042.

42. Mapossa AB, Dantas J, Diniz VCS, Costa ACFM, Silva MR, Kiminami RHGA. Synthesis and characterization of $Ni_{0.7}Zn_{0.3}Fe_2O_4$ ferro spinel: performance evaluation for methyl and ethyl esterification. Ceramica. 2017. 63(366), 223-232.

43. Vahid BR, Haghighi M. Biodiesel production from sunflower oil over $MgO/MgAl_2O_4$ nanocatalyst: effect of fuel type on catalyst nanostructure and performance. Energy Conversion and Management. 2017; 134, 290-300.

44. Sheoran A, Dhiman M, Bhukal S, Malik R, Agarwal J, Chudasama B, Singhal S. Development of magnetically retrievable spinel nanoferrites as efficient catalysts for aminolysis of epoxides with amines. Materials Chemistry and Physics. 2019; 222, 207-216.